Sains Malaysiana 53(3)(2024): 705-717
http://doi.org/10.17576/jsm-2024-5303-17

Effect of Short Heat Treatments on the Microstructural Evolution and Hardness of Thixoformed Graphene Reinforced Aluminium Composites

(Kesan Rawatan Haba Singkat terhadap Evolusi Mikrostruktur dan Kekerasan Komposit Aluminium Diperkuat Grafen Pembentukan Tikso)

Nur Farah Bazilah Wakhi Anuar[1,2], Mohd Zaidi Omar[1], Mohd Shukor Salleh[2,*], Wan Fathul Hakim W. Zamri[1] & Afifah Md Ali[1]

[1]*Department of Mechanical and Manufacturing Engineering, Faculty of Engineering and Built Environment, Universiti Kebangsaan Malaysia, 43600 UKM Bangi, Selangor, Malaysia*
[2]*Fakulti Teknologi dan Kejuruteraan Industri dan Pembuatan, Universiti Teknikal Malaysia Melaka, Hang Tuah Jaya, 76100 Durian Tunggal, Melaka, Malaysia*

Received: 26 September 2023/Accepted: 15 February 2024

ABSTRACT

Aluminium metal matrix composites are increasingly being used in numerous industries due to their lightweight nature and high strength. The incorporation of graphene into aluminium metal matrix composites has garnered significant interest owing to graphene's capacity to enhance numerous properties concurrently. Hence, this study aimed to fabricate a 0.3 wt.% graphene nanoplatelets reinforced A356 alloy (GNP-A356) composite through stir casting followed by thixoforming and short T6 heat treatment processes. It also evaluated the microstructure and mechanical properties of GNP-A356 after the thixoforming process and short T6 heat treatment. The microstructure of alloy and composite was confirmed by optical microstructure, field emission scanning electron microscopy images, and X-ray diffraction. Microstructure investigations demonstrate the impact of the stirring process on the structural transformation of the α-Al phase from the dendritic into a rosette-like and globular-like structure. The result also indicated that there was a transformation of eutectic silicon from the shape of a needle-like to spheroid structure after a short heat treatment, showing the efficiency of T6 heat treatment with a shorter time of solution treatment and ageing. Moreover, the increase in relative density and addition of reinforcement led to a significant increment in hardness. The result shows the hardness improved by 35.77% and 77.8% for as-cast and heat-treated composites, respectively, compared to A356 alloy.

Keywords: Aluminum alloy; aluminium matrix composite; graphene; short T6 heat treatment; Thixoforming

ABSTRAK

Penggunaan komposit matriks logam aluminium semakin meningkat dalam pelbagai industri kerana sifatnya yang ringan dan kekuatan yang tinggi. Penggabungan grafen ke dalam komposit matriks logam aluminium telah mendapat kepentingan yang ketara kerana keupayaan grafen dalam meningkatkan keupayaan pelbagai sifat secara serentak. Komposit matriks logam aluminium semakin meningkat dalam pelbagai industri kerana cirinya yang ringan dan kekuatan tinggi. Penggabungan grafen ke dalam komposit matriks logam aluminium telah menarik minat kerana keupayaan grafen meningkatkan pelbagai ciri secara serentak. Oleh itu, kajian ini bertujuan menghasilkan komposit aloi A356 diperkuat 0.3 bt.% grafen nanoplatelet (GNP-A356) melalui adukan tuangan diikuti dengan proses pembentukan-tikso dan rawatan haba T6 singkat. Kajian ini juga menilai mikrostruktur dan sifat mekanik GNP-A356 selepas pembentukan-tikso dan rawatan haba T6 singkat. Mikrostruktur dikaji menggunakan mikrostruktur optik, imej mikroskop elektron pengimbasan pelepasan medan, dan pembelauan sinar-X. Penyelidikan mikrostruktur menunjukkan kesan proses adukan ke atas transformasi struktur fasa α-Al daripada dendritik kepada struktur seakan roset dan sfera. Hasil kajian juga menunjukkan bahawa terdapat transformasi eutektik silikon daripada bentuk seakan jarum kepada struktur sferoid selepas rawatan haba singkat yang menunjukkan kecekapan rawatan haba T6 dengan masa larutan rawatan dan masa penuaan yang singkat. Selain itu, peningkatan dalam ketumpatan relatif dan penambahan tetulang membawa kepada peningkatan yang ketara dalam kekerasan Keputusan menunjukkan terdapat peningkatan kekerasan sebanyak 35.77% dan 77.8% untuk komposit tuangan dan komposit dirawat haba, masing-masing, berbanding aloi A356.

Kata kunci: Aloi aluminum; grafen; komposit matriks aluminium; pembentukan tikso; rawatan haba T6 singkat

INTRODUCTION

Nowadays, aluminium alloy is utilised extensively instead of conventional materials aluminium matrix composites to produce a variety of automotive and aerospace components (Akçamlı et al. 2022). Al-Si alloys with a high silicon content (4.0-13.0%) have an opportunity in the heavy transportation industry owing to their exceptional mechanical properties, lightweight, and high resistance toward corrosion and wear (Abboud & Mazumder 2020; Arriaga-Benitez & Pekguleryuz 2023; Dwivedi, Sharma & Mishra 2014), and suitable for application in automotive structural parts such as engine pistons, connecting rods, cylinder liners and piston rings (Akçamlı et al. 2022; Jiang et al. 2022). Generally, ceramic-based particles such as Al_2O_3, SiC, TiB, and B_4C were introduced as reinforcement materials into the aluminium matrix to enhance the mechanical strength and tribological behaviour depending on the required parts or applications (Boppana et al. 2020; Leng et al. 2021). On the other hand, graphene has recently been recognised as a promising high-performance reinforcement material in aluminium matrix composites.

Graphene has received increasing recognition as a reinforcement material due to its remarkable physical and mechanical properties, including a large surface area of 2630 m^2g^{-1}, outstanding thermal conductivity of 5000 $Wm^{-1}K^{-1}$, excellent Young's modulus of 1 TPa and good ultimate tensile strength of 130 GPa (Güler & Bağcı 2020; Prashantha Kumar & Anthony Xavior 2017; Sadhu, Mandal & Sahoo 2023). In addition, the 2D-like structure of graphene and its much lower production cost than carbon nanotubes, creates an excellent alternative as a strengthening material for composites (Leng et al. 2021). Venkatesan and Anthony Xavior (2018) reported the mechanical behaviour of graphene reinforced AA7050 aluminium alloy with different graphene content (0.3, 0.5 and 0.7 wt.%). The tensile strength was enhanced at 0.3 wt.% GNP and then deteriorated with increasing graphene content at 0.5 wt.% GNP. Naik et al. (2022) fabricated the aluminium reinforced with graphene at four weights (1, 2, 3, 4 and 5 wt.%). There was an increase of 29.61% in hardness properties at 4 wt.% graphenes compared to as-cast aluminium. However, the hardness properties started to diminish after 5 wt.% owing to the graphene agglomeration in the aluminium matrix. Khanna et al. (2023) found the transformation of mechanical properties when adding different GNP contents to aluminium. It demonstrated that the hardness and compressive strength initially increased to 0.5 wt.% GNP and decreased after adding 1.0 wt.% GNP.

Various studies generally employed different fabrication strategies for producing graphene-reinforced aluminium matrix composites (Boppana et al. 2020). The powder metallurgy process is more widely applied in developing composites than the casting process because of its ability to uniformly distribute reinforcement particles in the metal matrix (Hanizam et al. 2020). However, applying the powder metallurgy technique to large-scale industry is not practical due to limitations in producing a component that requires a complex shape or high volume (Grilo et al. 2021). The employment of the casting process has gained as an option process to produce graphene-reinforced aluminium metal matrix composites, but there is a limitation with the casting process in the fabrication of graphene-reinforced metal composites. The graphene frequently tends to float on top of melt metal and increases the agglomeration of the reinforcement in the composites after it solidifies. Hence, the stirring operation in the casting route is applied with controlled parameters to generate a vortex state in the liquid metal matrix to assist in distributing the reinforcement particles in the metal matrix.

Furthermore, the thixoforming is one of the semi-solid techniques that can produce components with low porosity and less gas entrapment at semi-solid temperatures (Arendarchuck, Fals & Lourençato 2023; Talangkun, Potisawang & Saenpong 2020). The billet of semi-solid material with thixotropic properties experiences the shear force and produces the thixoformed billet with the detachment of dendritic arms with a multiplied grain (Arif et al. 2020; Putra, Manaf & Prajitno 2022; Samat et al. 2021). Md Ali et al. (2022) employed the thixoforming process to fabricate a GNP-reinforced A356 matrix composite. Their results indicate that applying the thixoforming process increased the relative density of the composite and significantly enhanced its mechanical properties. Wang, Chen and Pu (2022) successfully fabricated graphene oxide (GO) reinforced metal matrix composites through powder thixoforming. They reported that the structural integrity of GO was well maintained, and the ductility with hardness properties was enhanced after the thixoforming process.

The heat treatment substantially impacts the microstructures, and the mechanical properties of composites can be enhanced with appropriate heat treatments (Afifi et al. 2018). Heat treatment assists in the dissolving of the soluble phases such as Mg_2Si and β-Fe rich into a solid solution, homogenisation of alloy element and spheroidization of eutectic Si during treatment (Becker et al. 2022; Hanizam et al. 2019). Kim et al. (2021) identify the T6 heat treatment process enhanced the mechanical properties of A356 alloy owing to the homogeneous distribution of sphreroidisation Si and participation of required intermetallic compound. Gecu et al. (2018) conducted the T6 heat treatment on thixoforged A356 and A380 samples. They identified the increasing hardness values due to the Si uniform distribution, and the presence of Mg_2Si precipitates inside α-Al matrix. The several researchers have endeavoured to change the established T6 standard parameter to promote the dissolving process and facilitating the homogenisation of eutectic phases. Vanzetti et al. (2021) applied a short solution treatment of 540 °C for 15 min, water quench and artificial ageing at 170 °C for 6 h on AlSi7Mg alloy. The eutectic Si network transformed to globularisation and the micrometric of Si particles distributed homogeneously in the α-Al phase. In addition, the observation shows that the globular Si dimension was reduced to 1-2 μm, and it is almost similar to the full standard T6 heat treatment and the UTS, yield strength and elongation for short heat treatment by 14.3%, 27.7% and 25%, respectively, more than standard T6 heat treatment. Li, Zhang and Geng (2019) identified that the optimised temperature of heat treatment at 650 °C for 30 min successfully enhances the tensile strength of GNP-reinforced aluminium composite. The microstructure of α-Al in the composite matrix becomes coarser after the treatment but smaller than that of treated base aluminium. The hindering effect of GNP along the grain boundaries during short treatment affects it, and the Fe-rich phase changes to a particle-like shape.

There are various past studies on graphene-reinforced aluminium matrix composites, and obtaining a uniform graphene distribution throughout the aluminium matrix via the casting process is challenging. In addition, there is a limited and arduous understanding of the effect of combining the thixoforming process and heat treatment technique on the behaviour of graphene-reinforced aluminium matrix composite. Hence, this study aimed to produce GNP-reinforced A356 aluminium composites using stir casting followed by a semi-solid process and a short heat treatment technique. In addition, experimental work was also carried out to evaluate the effect of each process on the microstructure features and hardness properties of composites.

Materials and Methods

The alloy used for this process was commercial A356 aluminium alloy in the form of an ingot, and its chemical composition by weight percentage (Si - 7.38%, Mg - 0.26%, Cu - 0.0463%, Fe - 0.25%, Mn, - 0.190%, Zn - 0.0068%, Ti - 0.0411%) was obtained using the spectrometry technique. The GNP as a reinforcement material was obtained from Sigma-Aldrich, USA, with particle size <2 μm, a few nm of average thickness and greater than 95% purity. The 400 g of A356 aluminium alloy was heated in an induction furnace at 700 ºC until entirely melted. After it fully melted, the temperature was cooled to 650 ºC before the wrapping of preheated GNP (0.3 wt.%) and Mg powder (1.0 wt.%) were injected by a plunger to the base of the crucible. The Mg powder (Sigma-Aldrich, USA, with >99% purity) was added to enhance the wettability between the reinforcement and matrix. The three-blade stainless-steel stirrer was immediately placed in crucible and begin to stir the composite melt at approximately 500 rpm for 5 min. The medium speed was applied to prevent the air entrapment and restrict the development of high porosity in the composite (Hanizam et al. 2019). The melted mix was poured directly and solidified in a steel mould with a cylindrical shape.

Differential scanning calorimetry (DSC) analysis was conducted using a Mettler Toledo TGA/DSC in argon surrounding to estimate the liquid fraction profile range of the composites. The small piece of A356 alloy with less than 15 mg was heated to 700 °C at 10 °C/min. The small sample was exonerated in a nitrogen gas atmosphere to avoid oxidation. The cast composite billets with 120 × 30 mm Ø were placed in an induction coil with a high frequency of 30-80 kHz, 35 kW, under the mould to be heated to the 50% liquid-fraction temperature. The semi-solid temperature 581 °C was acquired based on the DSC curve as shown in Figure 1. The silicon mould release spray was applied on the die surface as a lubricant to minimise the adhesiveness between the samples and the mould surface. The composite billets were rammed into the mould with a load of 20 kN and speed of 85 $mm.s^{-1}$. The thermocouple (K-type) was used to monitor the heating temperature and removed from the semi-solid sample before the forging process. The thixoformed composites were removed from the die and allowed to cool at ambient temperature.

The short solution treatment was performed in the resistance furnace (Nabertherm 30 ºC - 3000 ºC) at 540 ºC for 1 h. The furnace was heated to a temperature of 540 ºC and held for 20 min before placing the thixoformed composites inside the furnace. After the short solution treatment, the samples were immediately quenched in 27 ºC water to preserve the desirable properties received

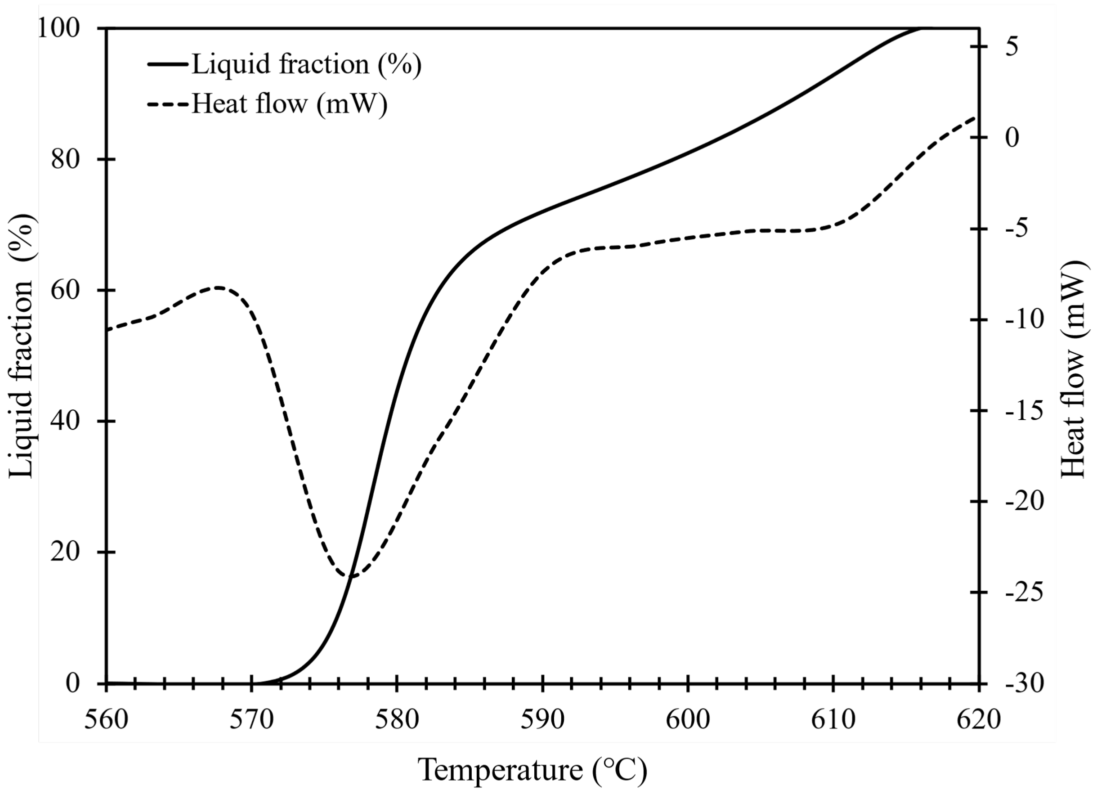

FIGURE 1. The liquid fraction and heat flow for A356 alloy

through heating. The quenched samples were transferred into the resistance furnace for artificial ageing at 180 ºC for 2 h and then cooled at room temperature.

The samples of A356 alloy, thixoformed composite and treated composite were cut and ground with P600, P800, P1000 and P1200 grinding paper. Subsequently, the ground samples were polished from 6 μm, 3 μm and up to 1 μm of diamond paste, followed by an etching process with Keller's reagent. The microstructure analysis of the composites was observed through an optical microscope (Nikon) and field emission scanning electron microscopy, FESEM (ZEISS Sigma 500, Germany). The intermetallic compounds were performed by energy dispersive spectroscopy (EDX) attached to FESEM. For X-ray diffraction analysis (XRD), the flatted samples were scanned at angles from 20 º and 90 º using Kα and Cu radiation sources. The hardness effect of thixoforming and short T6 heat treatment was analysed using the Vickers hardness test using VH testing Shimadzu machine according to ASTM E384 – 17 standards with 9.807 N test load and 10 s dwell time. Ten measurement points were measured and averaged for each Vickers hardness value.

Results and Discussion

Figure 2 shows the XRD pattern of A356 alloys and GNP-A356 composites with different process. It shows that the peaks of aluminium at [1,1,1], [2,0,0], [2,2,0], [3,1,1], and [2,2,2] corresponding to face-centered cubic crystal structure and peaks of silicon at [111], [2,2,0], and [311] for A356 alloy, as-cast GNP-A356 composite, thixoformed GNP-A356 composite and ST6 thixoformed GNP-A356 composite. Aluminium peaks were dominant in all A356 alloy and composite samples without any visible peak for GNP. The peaks of XRD for thixoformed composites were obtained, and the diffraction peaks were less intense possibly owing to the attachment and dispersion of GNP onto the aluminium matrix (Kabir et al. 2023). In addition, the non-appearance of GNP peaks for all composite samples can be ascribed to the low GNP content (Khanna et al. 2023; Lin et al. 2022; Wei et al. 2023). However, carbon (C) particles were detected at 43.61º [1,0,-1] for GNP-A356 composites at as-cast and thixoforming process. Moreover, the XRD identified the tiny Al_4C_3 diffraction peaks around 43.61º and 40.10º, indexed to [0,0,12] and [1,0,7], at as-cast and thixoformed composite, respectively. Şenel and Gürbüz (2020) reported there was no formation of Al_4C_3 between aluminium and carbon elements in Si_3N_4/GNPs reinforced aluminium composite fabricated by powder metallurgy. They were clarifying existence of carbide phase can deteriorate the structure of composite. Wang et al. (2019) avoided the appearance of Al_4C_3 during sintering from declining the performance of composites by employing the field activated and pressure-assisted synthesis in sintering process.

On the other hand, the formation of the compound Al_4C_3 in graphene-reinforced aluminium composites has been reported in several studies (Borand & Uzunsoy 2022; Han et al. 2020; Lin et al. 2023). Borand and Uzunsoy (2022) detect carbide phase formation in the composite produced by powder metallurgy in XRD and identify that interfacial phase of Al_4C_3 can provide good load transfer between aluminium matrix and graphene which hinders the movement of dislocation. In this study, the presence of Al_4C_3 demonstrating a slight interfacial interaction between carbon and aluminium during fabrication. In addition, it is known that graphene reacts with aluminium at temperatures above 500 °C (Zhang et al. 2022), and the formation of Al_4C_3 phase can be occurred between graphene and aluminium by reaction of $4Al(s)+3C(s) \rightarrow Al_4C_3$. Thus, it is possible Al_4C_3 is formed during the casting process. The presence of carbide phase can reduce the surface tension carbon and aluminium thus enhance the wettability between carbon and aluminium and improving the hardness of the composite (Spierings et al. 2023). Moreover, the small existence of Al_4C_3 usually contribute a pinning effect on the boundary of α-Al and inhibits grain development and prevents the movement at the grain boundary (Yehia, Nyanor & Daoush 2022). However, the excessive formation of brittle intermetallic compounds Al_4C_3 led to detrimental tendency in hardness of composite. Hence, controlling the amount of Al_4C_3 compound benefits the load transfer effect and enhances the strength of the composite (Han et al. 2021).

Other intermetallic phases of Mg_2Si at [2,0,0], [2,2,0], [3,1,1], [3,3,1], and [5,1,1] and $Al_8Si_6Mg_3Fe$ at [2,0,2], [0,0,4], [2,0,4], [1,1,5], and [3,2,2] were detected in samples. The formation of intermetallic compounds at grain boundaries is crucial in enhancing bonding strength between the grains in the composite. Fe-rich intermetallic phases of Al_5FeSi were detected at [1,1,9], [0,3,2] and [3,4,1] for alloy A356, while it was detected at [1,1,9] and [3,2,-7] for as-cast composite, [1,1,19] for thixoformed composite, and [0,0,19] and [1,1,19] for thixoformed ST6 composite.

Figure 2 also illustrates the XRD peaks of ST6-thixoformed GNP-A356 composite composites shifted to the lower diffraction angle in comparison to the A356 alloy and non-heated composites' diffraction peaks. The transformation microstructure of composites, including changes in crystal structure and expansion in the lattice, can affect the shifted diffraction peak for the ST6-thixoformed GNP-A356 composite. Heat treatment in a short time can also relate to the residual stress of the composite, affecting the diffraction (Chen et al. 2021) in a short time and it affects the diffraction angle.

Figure 3(a) shows the received microstructure of A356 alloy under the optical microstructure. The microstructural features throughout the sample show the common α-Al with dendritic structure and interdendritic needle-like structures of the Si eutectic. Figure 3(b) shows the apparent changes in microstructural features of the GNP-A356 composite in the primary phase morphology after the stirring activity. The dendritic structure was transformed into a non-uniform α-Al rosette-like and almost globular structure. The structural transformation is the resulted from vortex mechanical forces where the external forces break the dendritic arms and form the island. In addition, the phenomenon of vortex formation resulting from solid-liquid mixing facilitates the transfer of reinforcement particles from the liquid surface into the melt. Concurrently, the shearing action disrupt the accumulation of reinforcement particles, thereby promoting a homogeneous distribution. However, the disturbance of the formation uniform globular microstructure was caused by the combined inertia of the turbulent during stirring and the inertia of reinforcement particles in the melt. Nevertheless, this outcome is adequate for the subsequent thixoforming process (Hanizam et al. 2019). Thixoforming was performed by applying a compression press on the composite material after reheating it at semi-solid temperatures. The morphology of the thixoformed composite showed a growth of nearly globular and coarsened α-Al grains, as shown in Figure 3(c). The adjacent α-Al amalgamation happened during the initial stages of the heating process or at a low liquid fraction. During this phase, most of the small α-Al globules possessing high interfacial energy

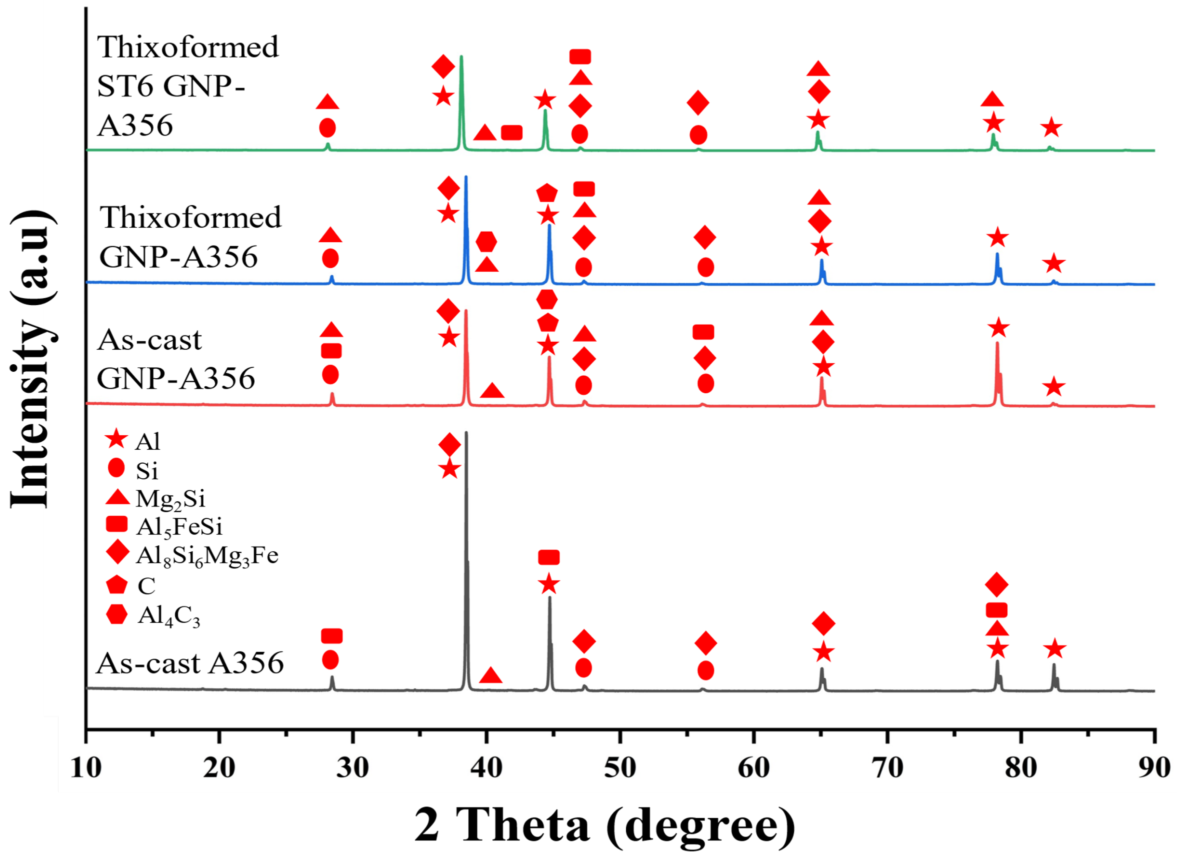

FIGURE 2. XRD patterns of the A356 alloy and 0.3 wt.% GNP-reinforced A356 composite with a different process

congregated into larger globules. The coarsening of α-Al was also facilitated by coalescence and Ostwald ripening mechanisms. Furthermore, it also shows that Si eutectic was entrapped into the globules of α-Al after thixoforming. However, some needle-like Si particles had fragmented into plate-like and polyhedral structures around the globules of α-Al owing to the rearrangement position of remelted eutectic Si during the reheating process. Hence, the thixoforming process not only modified the morphology of α-Al with rearrangement and transformation of needle-like Si to enhance the mechanical properties of the composite but also decrease the porosity of the composite (Abdelgnei et al. 2019). Figure 3(d) shows the microstructure with further globules α-Al coarsening in the composite after a short T6 heat treatment. Moreover, the entire eutectic Si elements had transformed from needle-like into a spheroidal structure after being subjected to heat treatment. In addition, the Si particles uniformity was enhanced after a short T6 heat treatment, resulting in anticipated improvements of the thixoformed composite.

Figure 4 shows the FESEM morphologies of the composites for as-cast, thixoformed and thixoformed short T6 heat treatment. Three types of intermetallic phases of β-Al_5FeSi, π-$Al_8FeMg_3Si_6$, and Mg_2Si were formed in the composites. The presence of a Fe-rich needle-like intermetallic compound was detected in the microstructure of as-cast A356. There was transformation of some needle-like β-Al_5FeSi in Figure 4(a) to polyhedral-like after applying the thixoforming process as shown in Figure 4(b) for composite samples. However, a needle-like β-Al_5FeSi still existed in the eutectic Si after

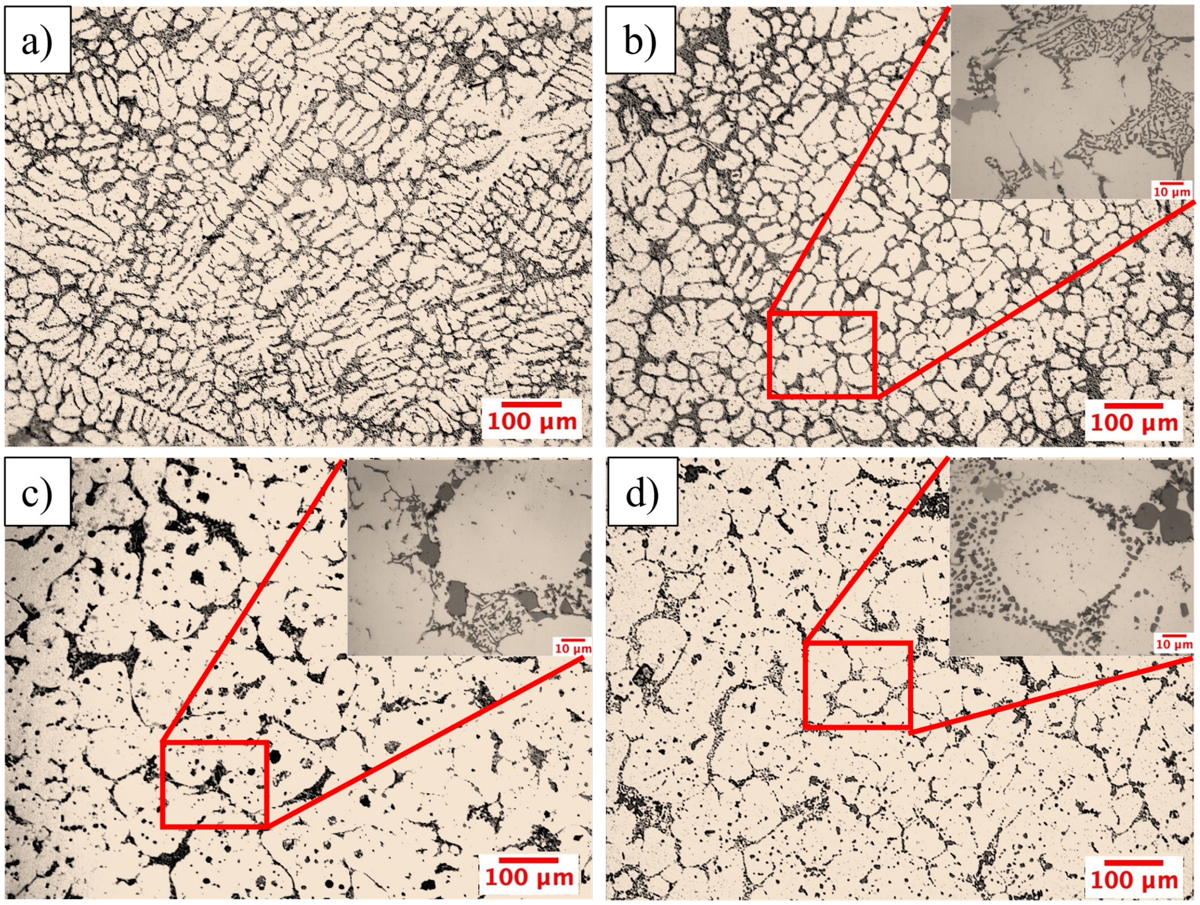

FIGURE 3. The optical microscope for the microstructure of (a) as-cast A356 alloy without stirring, (b) as-cast GNP-A356 composite, (c) thixoformed GNP-A356 composite, and (d) thixoformed-ST6 GNP-A356

undergoing the short T6 heat treatment owing to the high melting temperature of Fe-rich intermetallic phase as low as 615 °C (Song et al. 2020) compared to the temperature used in short T6 treatment that can diminish the composite strength. Nevertheless, Fe is known to improve the thermal stability of aluminum alloys due to its low diffusion coefficient, but the presence of uncontrolled Fe-rich intermetallic compound can degrade the hardness of the material (Liu et al. 2020; Novák et al. 2023). The addition of GNP controls the nucleation of the Fe-rich during short T6 heat treatment due to limited growing space and converting the harmful Fe-rich into a less detrimental form. There was also the π-phase observation where π-$Al_8FeMg_3Si_6$ existed as compact morphology and was less detrimental than the β-Al_5FeSi as shown in Figure 4(c) for thixoformed heat-treated composite. This contrasted the as-cast composite where π-$Al_8FeMg_3Si_6$ formed as needle-like structure, as shown in Figure 4(a), reduces the hardness of the composite. After a short T6 heat treatment, the particle distribution Si improved, and the particles entirely transfigured into the spheroidal structure, as mentioned earlier. It even demonstrated the growth of two nearby eutectic silicon particles and increased eutectic silicon size, as shown in Figure 4(c).

Nevertheless, the precipitation of Mg_2Si in small formations alongside the silicon particles as homogeneously distributed in the entire composite. This formation assisted in enhancing the hardness properties of the composite. Therefore, physical changes and integration between the soluble phase and reinforcement GNP in microstructure can be achieved and sufficiently in 1 h solution treatment. The changes in short-duration treatment led to a significant impact in enhancing the mechanical properties to the maximum.

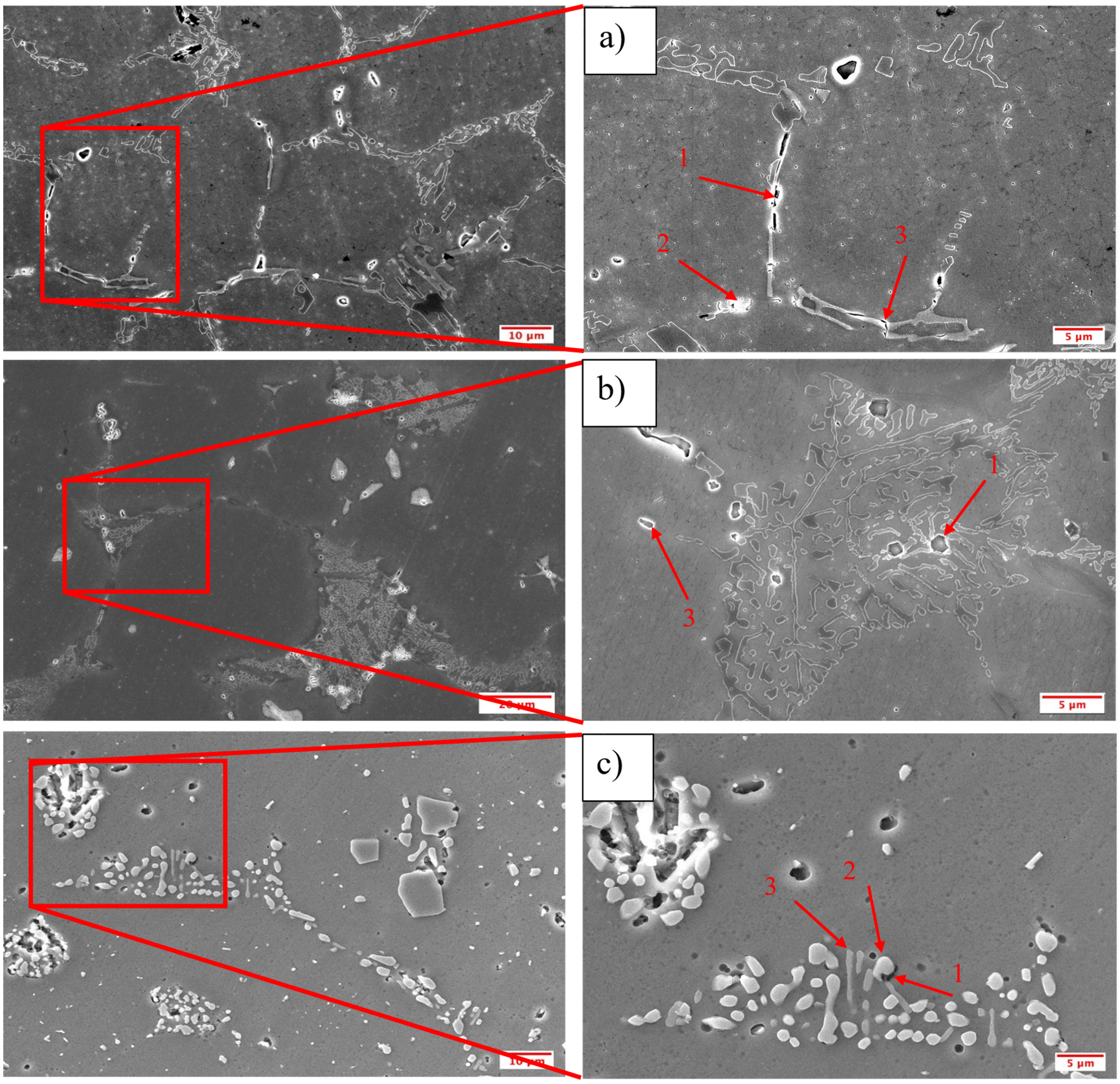

FIGURE 4. Field emission scanning electron microscopy (FESEM) micrographs showing the morphology of (a) as-cast 0.3 wt.% GNP-A356, (b) thixoformed GNP-A356 composite, and (c) thixoformed-ST6 GNP-A356. (arrow 1: $AlFe_5Si$, 2: Mg_2Si, 3: $Al_8FeMg_3Si_6$)

Table 1 shows the density description and experimental density values of GNP-A356 composites for each processing and base alloy as reference samples, respectively. The experimental density was measured using the Archimedes rule, while the relative density was represented by the experimental density to theoretical density ratio from the rule of mixture. The as-cast of GNP-A356 composite decreases compared to base alloy of A356 owing to the significant difference in density between GNP and A356 alloy. The density of GNP-A356 composite tends to decrease because GNP is lighter than aluminium (Khan et al. 2019). Moreover, the reduction in density of the as-cast composite can be attributed to interstitial voids within clusters and the discontinuity defect such as shrinkage during solidifications and gas entrapment during stirring (Abbasipour et al. 2019).

Hence, combining different density of reinforcement and aluminium, and the presence of porosity during solidification reduces the density of the composite compared to the base alloy. However, the thixoforming process method affects the density of the composite owing to compressing pressure on the composite in semi-solid condition and promote the densification of the composites. In addition, the lubricating effect of GNP can facilitate flowability improvement of the composite during compression in semi-solid conditions, resulting in a descending trend of porosity and increasing the hardness of the composite (Chen et al. 2023). This showed that the relative density was one of the crucial elements in enhancing the hardness of the GNP-A356 composites.

Figure 5 shows the hardness values of A356 alloy and GNP-A356 composites. GNP-A356 composites exhibited a rapid hardness increase after adding the reinforcement, and their hardness increased gradually after thixoforming and a short T6 heat treatment. GNP incorporation in A356 substantially increase the hardness of the produced composites by 35.77% compared to A356 alloy (63.01 ± 6.55 HV). The substantial hardness improvement caused by adding a sufficient GNP quantity can be associated with the homogeneous distribution of reinforcement grains throughout the A356 matrix (Khanna et al. 2023). It also shows that the hardness of the thixoformed composite sample subsequently increased and was higher than those of the corresponding as-cast of GNP-A356 composite. This is due to a combination of defects reduction such as porosity and shrinkage in thixoformed composite samples, homogeneous distribution of reinforcement in the matrix and characteristic of GNP. Furthermore, the hardness value of the GNP-A356 composite reached the maximum value after a short heat treatment (112.05 ± 4.97 HV) compared to the thixoformed GNP-A356 composite (95.39 ± 3.7HV). This result was consistent with Cai et al. (2020), that short heat treatment increased the hardness value and minimised the expansion of porosity. Hence, only 1 h solution treatment with 2 h ageing enhanced the hardness of the thixoformed composite compared to the as-cast and thixoformed composites. Furthermore, the solution treatment in a short time allows Mg dissolution and transformation of eutectic Si to form a spheroidal structure. It also combined with the growth controlled of α-Al grains and the limited nucleation of the Fe-rich phase due to blocking by GNP. In addition, the increase of hardness may also be concluded from the precipitation and distribution of fine Mg_2Si after short T6 heat treatment. Furthermore, the superior mechanical characteristics possessed by graphene offered the necessary force to inhibit the distortion during the indentation, which improved the hardness of GNP-A356 composites (Azizi, Rahmani & Taheri-Behrooz 2022).

Table 2 compares the hardness properties of the composites studied in this work and other research data by adding graphene as reinforcement in aluminium alloy. From Table 2, some hardness is higher than the hardness values in this work because of the limited content of reinforcement. In addition, the hardness properties of this work were higher than those of some other research. This is probably due to the application of the thixoforming process and a good distribution of reinforcement material.

TABLE 1. Density description of base alloy and GNP-A356

Description	Experimental density (g/cm^3)	Theoretical density (g/cm^3)	Relative density (%)
As-cast A356	2.6790 ± 0.0010	2.7000	99.222
As-cast GNP-A356	2.6780 ± 0.0018	2.6980	99.259
Thixoformed GNP-A356	2.6880 ± 0.0015	2.6980	99.640
Thixoformed-ST6 GNP-A356	2.6940 ± 0.0011	2.6980	99.852

Second, the changes in silicon element structure from a fibrous structure to a spheroid structure microstructure after a short T6 heat treatment process. The exact mechanism behind the improvement in hardness after the heat treatment process probably involves grain Orowan strengthening mechanisms, stress load transfer, and thermal expansion mismatches (Li, Zhang & Geng 2019). However, the transformation structure of silicon elements in composites significantly contributes to the strengthening mechanism of composites after a short T6 heat treatment process. Therefore, compared with other types of fabrication processes, the modified short solution and ageing treatments could be promising because they could become enormously beneficial in terms of production cost and time, with almost the same mechanical properties as previous research.

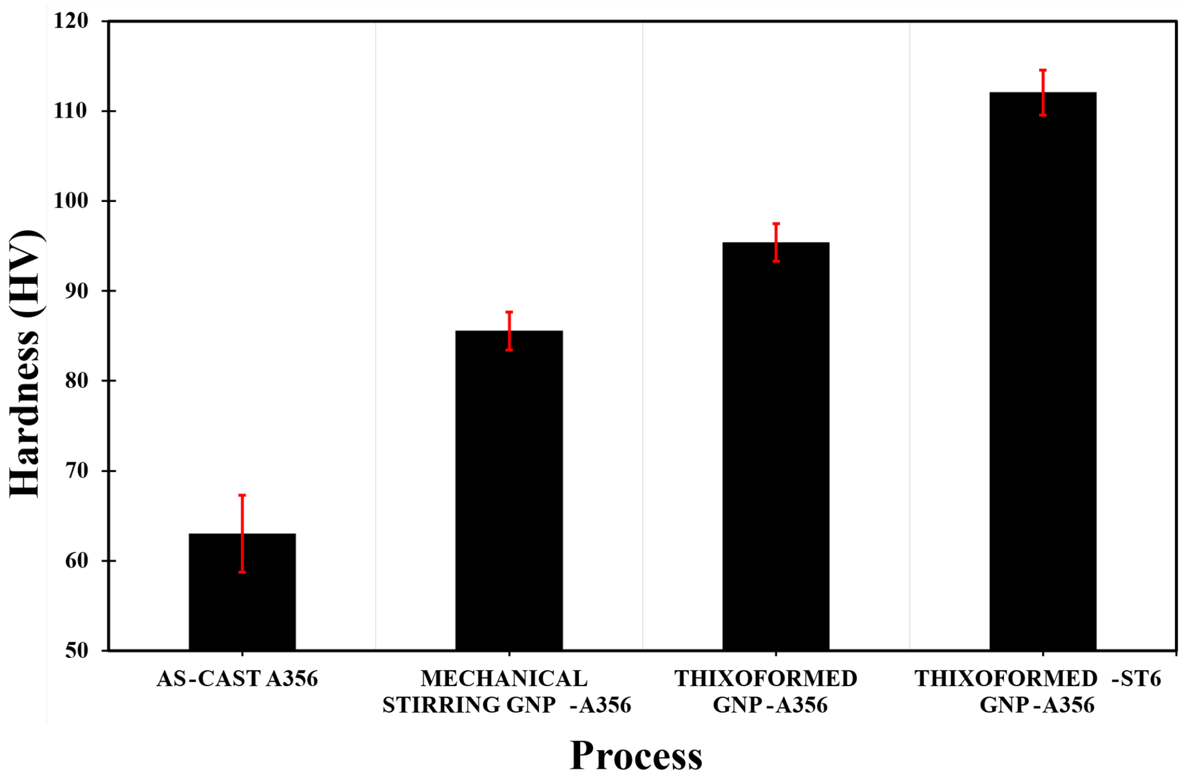

FIGURE 5. Hardness of A356 alloy and GNP-A356 composites for each process

TABLE 2. Comparison of hardness properties of graphene-reinforced aluminium alloy

Composite	Process	Hardness	Ref.
0.3 wt.% GNP/A356	Stir casting + Thixoforming + Short T6 heat treatment	112.05 ± 4.97 HV	This work
2 wt.% graphene/Al pure	Ball milling + Laser powder bed fusion	137 HV	(Ghazanlou et al. 2023)
1.0 wt.% RGO/ Al-Mg-Si	Powder metallurgy	~97 HV	(Yang et al. 2023)
0.5 wt.% GNP/Al	Powder metallurgy	40.3 HV	(Khanna et al. 2023)
GNP/AA5083	Friction stir processing	113 ± 3 HV	(Moustafa et al. 2022)
7.5 wt.% GNs/Al_2O_3/Al-Ni-Mg	Ball milling + Hot pressing	98 HV	(Yehia, Nyanor & Daoush 2022)
rGO/Al-Si (ADC12)	Gravity stir die-casting	~90 HV	(Singh et al. 2021)
0.5 wt.% GNP/Al	Powder metallurgy	73 HV	(Yu et al. 2021)

Conclusion

The work fabricated 0.3 wt.% GNP-A356 composite using stir casting assisted with thixoforming and a short T6 heat treatment technique. The effect on hardness properties and microstructures was investigated. Based on the results, the following conclusions can be drawn:

1) The XRD shows an Al_4C_3 formation resulting from the chemical reaction between GNP and A356 during fabrication, 2) The microstructure of α-Al was transformed to non-dendritic after stir casting process and become coarser after the thixoforming and short T6 heat treatment processes. The Si phase was transformed from fibrous structure to spheroids structure after the short T6 heat treatment, 3) FESEM shows the presence of other intermetallic compounds such as Mg_2Si, $Al_8FeMg_3Si_6$ and Al_5FeSi, which was significant to the strength of the composites, 4) The relative density of the GNP-A356 composite was improved after the thixoforming and short T6 heat treatment process, and 5) The hardness of the composite was enhanced by 35.77% after adding the GNP in the A356 alloy and 77.8% after the thixoforming and short T6 heat treatment process compared to the A356 alloy.

ACKNOWLEDGEMENTS

The study is funded by the Ministry of Higher Education (MOHE), Malaysia through the Fundamental Research Grant Scheme (FRGS), No. FRGS/1/2022/TK10/UTEM/02/18. The authors would also like to thank Universiti Teknikal Malaysia (UTeM) and Universiti Kebangsaan Malaysia (UKM) for supporting this study.

REFERENCES

Abbasipour, B., Niroumand, B., Monir Vaghefi, S.M. & Abedi, M. 2019. Tribological behavior of A356−CNT nanocomposites fabricated by various casting techniques. *Transactions of Nonferrous Metals Society of China* 29(10): 1993-2004.

Abboud, J. & Mazumder, J. 2020. Developing of nano sized fibrous eutectic silicon in hypereutectic Al–Si alloy by laser remelting. *Scientific Reports* 10(1): 12090.

Abdelgnei, M.A.H., Zaidi Omar, M., Ghazali, J., Gebril, M.A. & Mohammed, M.N. 2019. The effect of the rheocast process on the microstructure and mechanical properties of Al-5.7Si-2Cu-0.3Mg alloy. *Jurnal Kejuruteraan* 31(2): 317-326.

Afifi, M.A., Wang, Y.C., Pereira, P.H.R., Huang, Y., Wang, Y., Cheng, X., Li, S. & Langdon, T.G. 2018. Mechanical properties of an Al-Zn-Mg alloy processed by ECAP and heat treatments. *Journal of Alloys and Compounds* 769: 631-639.

Akçamlı, N., Şenyurt, B., Gökçe, H. & Ağaoğulları, D. 2022. Powder metallurgical fabrication of graphene reinforced near-eutectic Al-Si matrix composites: Microstructural, mechanical and electrochemical characterization. *Engineering Science and Technology, an International Journal* 31: 101052.

Arendarchuck, B.E., Fals, H.D.C. & Lourençato, L.A. 2023. Effect of thixoforming process and microstructural changes in the A380 matrix composite reinforced with NbC by the stir casting method. *JOM* 75(1): 184-194.

Arif, M.A.M., Omar, M.Z., Sajuri, Z. & Salleh, M.S. 2020. Effects of Cu and Mg on thixoformability and mechanical properties of aluminium alloy 2014. *Transactions of Nonferrous Metals Society of China* 30(2): 275-287.

Arriaga-Benitez, R.I. & Pekguleryuz, M. 2023. The synergistic effects of nano-sized α-Al(Mn,Cr,Fe)Si and Al–Si–Zr dispersoids on the creep behavior Al–Si–Mg–Cu (Mn, Cr, Zr) diesel engine alloy. *Materials Science and Engineering: A* 872: 144949.

Azizi, Z., Rahmani, K. & Taheri-Behrooz, F. 2022. The influence of graphene nanoplatelets addition on the electrical and mechanical properties of pure aluminum used in high-capacity conductors. *Metals* 12(11): 1883.

Becker, H., Bulut, N., Kortus, J. & Leineweber, A. 2022. β-Al4.5FeSi: Hierarchical crystal and defect structure: Reconciling experimental and theoretical evidence including the influence of Al vs. Si ordering on the crystal structure. *Journal of Alloys and Compounds* 911: 165015.

Boppana, S.B., Dayanand, S., Anil Kumar, M., Kumar, V. & Aravinda, T. 2020. Synthesis and characterization of nano graphene and ZrO2 reinforced Al 6061 metal matrix composites. *Journal of Materials Research and Technology* 9(4): 7354-7362.

Borand, G. & Uzunsoy, D. 2022. Fabrication of functionally graded few-layered graphene reinforced Al-4.5Cu alloy by powder metallurgy. *Journal of Alloys and Compounds* 923: 166348.

Cai, Q., Mendis, C.L., Chang, I.T.H. & Fan, Z. 2020. Effect of short T6 heat treatment on the microstructure and the mechanical properties of newly developed die-cast Al–Si–Mg–Mn alloys. *Materials Science and Engineering: A* 788: 139610.

Chen, L., Zhao, Y., Jing, J. & Hou, H. 2023. Microstructural evolution in graphene nanoplatelets reinforced magnesium matrix composites fabricated through thixomolding process. *Journal of Alloys and Compounds* 940: 168824.

Chen, Y., Wang, L., Feng, Z. & Zhang, W. 2021. Effects of heat treatment on microstructure and mechanical properties of SLMed Sc-modified AlSi10Mg alloy. *Progress in Natural Science: Materials International* 31(5): 714-721.

Dwivedi, S.P., Sharma, S. & Mishra, K.R. 2014. A356 Aluminum alloy and applications - A Review. *International Journal of Advanced Materials Manufacturing & Characterization* 4(2): 81-86.

Gecu, R., Acar, S., Kisasoz, A., Altug Guler, K. & Karaaslan, A. 2018. Influence of T6 heat treatment on A356 and A380 aluminium alloys manufactured by thixoforging combined with low superheat casting. *Transactions of Nonferrous Metals Society of China* 28(3): 385-392.

Ghazanlou, S.I., Ghazanlou, S.I., Ghazanlou, S.I., Hosseinpour, S., Liao, Y. & Javidani, M. 2023. Improving the properties of an Al matrix composite fabricated by laser powder bed fusion using graphene–TiO_2 nanohybrid. *Journal of Alloys and Compounds* 938: 168596.

Grilo, J., Carneiro, V.H., Teixeira, J.C. & Puga, H. 2021. Manufacturing methodology on casting-based aluminium matrix composites: Systematic review. *Metals* 11(3): 436.

Güler, Ö. & Bağcı, N. 2020. A short review on mechanical properties of graphene reinforced metal matrix composites. *Journal of Materials Research and Technology* 9(3): 6808-6833.

Han, T., Wang, F., Li, J., He, C. & Zhao, N. 2021. Effect of GNPs on microstructures and mechanical properties of GNPs/Al-Cu composites with different heat treatment status. *Journal of Materials Science and Technology* 92: 1-10.

Han, Y., Ke, Y., Shi, Y., Liu, Y., Yang, G., Li, Z., Xiong, D.B., Zou, J. & Guo, Q. 2020. Improved mechanical property of nanolaminated graphene (reduced graphene oxide)/Al–Mg–Si composite rendered by facilitated ageing process. *Materials Science and Engineering A* 787: 139541.

Hanizam, H., Salleh, M.S., Omar, M.Z. & Sulong, A.B. 2019. Effects of mechanical stirring and short heat treatment on thixoformed of carbon nanotube aluminium alloy composite. *Journal of Alloys and Compounds* 788: 83-90.

Hanizam, H., Salleh, M.S., Omar, M.Z., Sulong, A.B. & Arif, M.A.M. 2020. Effects of hybrid processing on microstructural and mechanical properties of thixoformed aluminum matrix composite. *Journal of Alloys and Compounds* 836: 155378.

Jiang, J., Yan, J., Liu, Y., Hu, G., Wang, Y., Ding, C. & Zou, D. 2022. Investigation on heat treatment of large-sized and complex AlSi9Mg aluminum alloy components formed by squeeze casting. *Journal of Alloys and Compounds* 924: 166504.

Kabir, H., Munir, K., Wen, C. & Li, Y. 2023. Microstructures, mechanical and corrosion properties of graphene nanoplatelet–reinforced zinc matrix composites for implant applications. *Acta Biomaterialia* 157: 701-719.

Khan, M., Ud Din, R., Wadood, A., Syed, W.H., Akhtar, S. & Aune, R.E. 2019. Effect of graphene nanoplatelets on the physical and mechanical properties of Al6061 in fabricated and T6 thermal conditions. *Journal of Alloys and Compounds* 790: 1076-1091.

Khanna, V., Kumar, V., Bansal, S.A., Prakash, C., Ubaidullah, M., Shaikh, S.F., Pramanik, A., Basak, A. & Shankar, S. 2023. Fabrication of efficient aluminium/graphene nanosheets (Al-GNP) composite by powder metallurgy for strength applications. *Journal of Materials Research and Technology* 22: 3402-3412.

Kim, W., Jang, K., Ji, C. & Lee, E. 2021. Effects of heat treatment on the microstructure and hardness of A356 (AlSi7Mg0.3) manufactured by vertical centrifugal casting. *Applied Sciences* 11(23): 11572.

Leng, J., Ren, B., Jin, Y., Zhu, Y. & Wang, K. 2021. Effects of graphene addition on the refinement of silicon phase in graphene/A356.2 composites. *Materials Letters* 292: 129610.

Li, J., Zhang, X. & Geng, L. 2019. Effect of heat treatment on interfacial bonding and strengthening efficiency of graphene in GNP/Al composites. *Composites Part A: Applied Science and Manufacturing* 121: 487-498.

Lin, F., Jia, F., Ren, M., Wang, J., Yang, M., Chen, Z. & Jiang, Z. 2022. Microstructure, mechanical and thermal properties of ultrafine-grained Al2024–TiC-GNPs nanocomposite. *Materials Science and Engineering: A* 841: 142855.

Lin, F., Ren, M., Wu, H., Jia, F., Lu, Y., Huo, M., Yang, M., Chen, Z. & Jiang, Z. 2023. Investigation of microstructure and tribological performances of high-fraction TiC/graphene reinforced self-lubricating Al matrix composites. *Tribology International* 177: 108018.

Liu, T., Karkkainen, M., Nastac, L., Arvikar, V., Levin, I. & Brewer, L.N. 2020. Iron-rich intermetallics in high pressure die cast A383 aluminum alloys. *Intermetallics* 126: 106814.

Md Ali, A., Omar, M.Z., Salleh, M.S., Hashim, H., Mohamed, I.F. & Wakhi Anuar, N.F.B. 2022. Mechanical behaviour and morphology of thixoformed aluminium alloy reinforced by graphene. *Materials* 15(19): 6791.

Moustafa, E.B., Melaibari, A., Alsoruji, G., Khalil, A.M. & Mosleh, A.O. 2022. Tribological and mechanical characteristics of AA5083 alloy reinforced by hybridising heavy ceramic particles Ta_2C & VC with light GNP and Al_2O_3 nanoparticles. *Ceramics International* 48(4): 4710-4721.

Manjunath Naik, H.R., Manjunath, L.H., Vinayak, M., Manjunath Patel, G.C., Saxena, K.K. & Anivash, L. 2022. Effect of microstructure, mechanical and wear on Al-CNTs/graphene hybrid MMC'S. *Advances in Materials and Processing Technologies* 8(Sup 2): 366-379.

Novák, P., Benediktová, D., Mestek, S., Tsepeleva, A. & Kopeček, J. 2023. Aluminum alloys with natural ratio of alloying elements manufactured by powder metallurgy. *Journal of Alloys and Compounds* 931: 167440.

Prashantha Kumar, H.G. & Anthony Xavior, M. 2017. Effect of graphene addition and tribological performance of Al 6061/graphene flake composite. *Tribology - Materials, Surfaces & Interfaces* 11(2): 88-97.

Putra, A.G., Manaf, A. & Prajitno, D.H. 2022. The effect of Ca and thixoforming process on hardness and microstructure of Mg–Al–Zn alloys. *Journal of Materials Research and Technology* 19: 643-652.

Sadhu, K.K., Mandal, N. & Sahoo, R.R. 2023. SiC/graphene reinforced aluminum metal matrix composites prepared by powder metallurgy: A review. *Journal of Manufacturing Processes* 91: 10-43.

Samat, S., Omar, M.Z., Baghdadi, A.H., Mohamed, I.F. & Aziz, A.M. 2021. Mechanical properties and microstructures of a modified Al–Si–Cu alloy prepared by thixoforming process for automotive connecting rods. *Journal of Materials Research and Technology* 10: 1086-1102.

Şenel, M.C. & Gürbüz, M. 2020. Microstructure and wear behaviour of graphene–Si_3N_4 binary particle-reinforced aluminium hybrid composites. *Bulletin of Materials Science* 43(1): 148.

Singh, H., Kumar, S., Kumar, D., Srivastav, M., Kumar, R., Jain, J., Chouhan, A. & Khatri, O.P. 2021. Reinforcing the near eutectic aluminum–silicon alloy with graphene: An approach toward self-lubricating composite. *Advanced Engineering Materials* 23(3): 2000910.

Song, D., Wang, S., Zhao, Y., Liu, S., Du, Y., Kang, Y., Wang, Z. & Zhang, W. 2020. Effect of melt holding on morphological evolution and sedimentation behavior of iron-rich intermetallic phases in Al—Si—Fe—Mn—Mg alloy. *Transactions of Nonferrous Metals Society of China* 30(1): 1-13.

Spierings, A.B., Ozherelkov, D.Y., Kneubühler, F., Eremin, S.A., Pelevin, I.A., Nalivaiko, A.Y., Petrov, E.A., Gromov, A.A. & Wegener, K. 2023. Laser powder bed fusion of AlSi10Mg-based composites with graphene and nanodiamond additions. *Journal of Alloys and Compounds* 947: 169421.

Talangkun, S., Potisawang, C. & Saenpong, P. 2020. Thixoforming and rheo-die-casting of A356/SiC composite. *Metals* 10(2): 251.

Vanzetti, M., Virgillito, E., Aversa, A., Manfredi, D., Bondioli, F., Lombardi, M. & Fino, P. 2021. Short heat treatments for the F357 aluminum alloy processed by laser powder bed fusion. *Materials* 14(20): 6157.

Venkatesan, S. & Anthony Xavior, M. 2018. Tensile behavior of aluminum alloy (AA7050) metal matrix composite reinforced with graphene fabricated by stir and squeeze cast processes. *Science and Technology of Materials* 30(2): 74-85.

Wang, J., Guo, L., Lin, W., Chen, J., Liu, C., Chen, S., Zhang, S. & Zhen, T. 2019. Effect of the graphene content on the microstructures and properties of graphene/aluminum composites. *New Carbon Materials* 34(3): 275-285.

Wang, L., Chen, T. & Pu, P. 2022. Synthesis of graphene oxide reinforced ZK60 magnesium matrix composite with high ductility via powder thixoforming. *Materials Science and Engineering: A* 830: 142307.

Wei, P., Chen, Z., Zhang, S., Li, B., Han, J. & Lu, B. 2023. Microstructure and mechanical properties of graphene and nano-zirconia reinforced AlSi10Mg composite fabricated by laser powder bed fusion. *Materials Science and Engineering: A* 864: 144574.

Yang, G., Han, Y., Liu, Y., Zheng, W., Ke, Y. & Guo, Q. 2023. Impact of graphene (reduced graphene oxide) incorporation on the aging behavior and mechanical properties of Al-Mg-Si alloy. *Materials Science and Engineering: A* 862: 144455.

Yehia, H.M., Nyanor, P. & Daoush, W.M. 2022. Characterization of Al-5Ni-0.5Mg/x (Al2O3-GNs) nanocomposites manufactured via hot pressing technique. *Materials Characterization* 191: 112139.

Yu, H., Zhang, S.Q., Xia, J.H., Su, Q., Ma, B.C., Wu, J.H., Zhou, J.X., Wang, X.T. & Hu, L.X. 2021. Microstructural evolution, mechanical and physical properties of graphene reinforced aluminum composites fabricated via powder metallurgy. *Materials Science and Engineering: A* 802: 140669.

Zhang, S., Wei, P., Chen, Z., Li, B., Huang, K., Zou, Y. & Lu, B. 2022. Graphene/ZrO_2/aluminum alloy composite with enhanced strength and ductility fabricated by laser powder bed fusion. *Journal of Alloys and Compounds* 910: 164941.

*Corresponding author; email: shukor@utem.edu.my